Integrodifferential formulations of the continuous-time random walk for solute transport subject to bimolecular $A + B \rightarrow 0$ reactions: From micro- to mesoscopic

Scott K. Hansen and Brian Berkowitz
Department of Earth and Planetary Sciences, Weizmann Institute of Science, Rehovot, Israel
(Received 31 July 2014; published 10 March 2015)

We develop continuous-time random walk (CTRW) equations governing the transport of two species that annihilate when in proximity to one another. In comparison with catalytic or spontaneous transformation reactions that have been previously considered in concert with CTRW, both species have spatially variant concentrations that require consideration. We develop two distinct formulations. The first treats transport and reaction microscopically, potentially capturing behavior at sharp fronts, but at the cost of being strongly nonlinear. The second, mesoscopic, formulation relies on a separation-of-scales technique we develop to separate microscopic-scale reaction and upscaled transport. This simplifies the governing equations and allows treatment of more general reaction dynamics, but requires stronger smoothness assumptions of the solution. The mesoscopic formulation is easily tractable using an existing solution from the literature (we also provide an alternative derivation), and the generalized master equation (GME) for particles undergoing $A + B \rightarrow 0$ reactions is presented. We show that this GME simplifies, under appropriate circumstances, to both the GME for the unreactive CTRW and to the advection-dispersion-reaction equation. An additional major contribution of this work is on the numerical side: to corroborate our development, we develop an indirect particle-tracking–partial-integro-differential-equation (PIDE) hybrid verification technique which could be applicable widely in reactive anomalous transport. Numerical simulations support the mesoscopic analysis.

DOI: 10.1103/PhysRevE.91.032113 PACS number(s): 02.50.Ey, 82.20.Wt, 05.40.Fb, 82.33.Ln

I. INTRODUCTION

A. Fundamentals

The continuous-time random walk (CTRW) formalism has proven to be a valuable tool in the modeling of both conservative and reversibly sorbing solute transport in heterogeneous media, underpinning both Eulerian (integrodifferential equation) and Lagrangian (particle tracking) approaches to transport modeling. More recently, there has been interest in modeling reactive transport, and Lagrangian CTRW-based computer models have been successfully applied to these problems. However, a corresponding Eulerian theory is desirable.

In an unreactive context, the CTRW equations are essentially a pair of convolution relationships relating two different quantities: $P_A(x,t)$ and $R_A(x,t)$. $P_A(x,t)$ is the amount of some species A at (discrete) site x at (continuous) time t, and $R_A(x,t)$ is the time rate of arrival of species A at site x at time t. It has been shown [1] that the following relations hold:

$$R_A(x,t) = \sum_{x'} \int_0^t \psi_A(x - x', t - t') R_A(x',t') dt', \qquad (1)$$

where $\psi_A(\Delta_x,\Delta_t)$ is a probability rate for transitions of length Δ_x made by a particle after delay Δ_t, and

$$P_A(x,t) = \int_0^t \Psi_A(t - t') R_A(x,t') dt', \qquad (2)$$

where we define $\Psi_A(\Delta_t) \equiv 1 - \sum_{\Delta_x} \int_0^{\Delta_t} \psi_A(\Delta_x,\tau) d\tau$ as the probability of the walker remaining at a given site for Δ_t. Our goal is to adapt these to a reactive context, where there is another species, B, whose movement is governed by its own ψ_B, and where particles that are "near" one another feature a probability of reaction that is nonzero. These modified equations have the potential to drive analysis of a variety of reactive solute transport phenomena at a variety of scales, including reaction rate reduction due to island formation at the pore scale, and the interplay of reaction and plume development in heterogeneous media at the bench and field scales.

The interplay of transport and reaction has been a topic of considerable recent research interest. Classically, $A + B \rightarrow C$ reactive transport has been considered by adding a nonlinear, "mass action law" reaction term of the form $\Gamma P_A P_B$ onto the governing transport equations that would obtain for P_A and P_B in the absence of reaction. It has long been recognized, however, that nonidealities are present, and that the combined effects of reaction and diffusion cause fronts to emerge that limit the rate of mixing, and thus reaction [2,3]. Many theoretical studies have examined the interplay of pure diffusion and reaction; considering the propagation of reaction fronts under various types of reaction, including $A + B \rightarrow 0$ [4] and $A + A \rightarrow 0$ [5]. More recently, new particle tracking methods have been developed for the diffusion-reaction equation [6,7], and the island formation behavior has been studied in detail.

B. Interplay of reaction and anomalous transport

Recent studies have also looked at how *anomalous* transport, in particular, affects the development of fronts under subdiffusion and types of reactions. These approaches have differed on whether they apply the anomalous transport operator to the mass action term [8] or not [9]. Other authors have considered (an $A + B \rightarrow 2A$ conversion) reaction under subdiffusion by means of asymptotic methods [10], and avoided explicitly formulating a governing anomalous reactive transport equation. Other recent works have examined the effects of superdiffusion on reaction by means of fractional spatial derivatives [11,12]. Another recent approach derives potentially anomalous governing equations for $A + B \rightarrow C$ reactions at the mesoscopic scale by upscaling ordinary diffusion-reaction equations at the pore scale [13,14].

 ©2015 American Physical Society

The above-mentioned works may be thought of as examinations of how transport, and particularly anomalous transport, affects reaction. At the same time, there has been interest in the converse phenomenon: the extent to which reaction influences anomalous transport. Many theoretical studies have called into question the use of a mass action term attached to the generalized master equation (or, in some cases, a fractional advection-dispersion equation) that would obtain in the unreactive case, contrary to some of the theoretical approaches mentioned above.

A common method for studying the effect of reaction on transport is to derive a CTRW-style integrodifferential generalized master equation (GME) that describes the overall probability (or equivalently, mass) dynamics in the system. This has the advantage of also illustrating how transport affects reaction, since the exact system dynamics are derived essentially from first principles. (For example, the front formation in the $A + B \to 2A$ reaction under subdiffusion mentioned above has been studied using such an approach [15], although without developing a closed-form solution.)

A number of works in this spirit have dealt explicitly with the case of first-order exponential decay, examining the interplay of transport and first-order, linear $A \to 0$ decay and subdiffusion, under different assumptions, including associating decay events with transitions [16] or alternatively with the time spent in waiting *between* transitions [17,18]. It is seen in the former case that the process can still be treated as a CTRW with an added reaction term, analogous to the ADE. Other authors considered the problems of first-order reversible $A \rightleftharpoons B$ reactions [19]. In all of these works, the governing equations remain linear, and so are amenable to solutions using the Laplace and Fourier-Laplace techniques that are employed to solve ordinary CTRW equations. These works show an interplay between reaction and transport, where the effect of reaction alters the transport term in the master equation, as well as adding an explicit decay term. A generalization to the decay expressions analyzed above was later developed when the probability of reaction over a transition from point x' and time t' to point x at time t can be expressed as a ratio $f(x,t)/f(x',t')$ for some arbitrary f [20].

In parallel, a number of studies have developed integrodifferential governing equations for anomalous diffusion in the presence of more general reaction terms, where the instantaneous rate of reaction is a function of one or more concentrations. In [21], the authors allowed an instantaneous reaction rate which was an arbitrary, not necessarily exponential, function of the time at a site, $f(t - t')$. More generally, [22] developed an integrodifferential governing equation for general multispecies nonlinear reactions that was not based on the usual CTRW relations, but rather based on an explicit particle age formulation due to [23]. Their formulation accounts for an instantaneous reaction rate of the form $f(P_A(x,t)P_B(x,t)\dots)$, for an arbitrary number of components and an arbitrary f. An alternative derivation employing the same age-based conception was also derived by [24] using a reaction model in which reaction is guaranteed whenever potentially reactive particles become adjacent.

Later, [25] enhanced the approach of [17] to account for arbitrary, nonlinear $A \to B$ conversion reactions, where the instantaneous reaction rate is $f(P_A(x,t))$, for some arbitrary f. Like [22], he succeeded in deriving an integrodifferential master equation, although this approach varied from that of the earlier paper in that waiting times were not reset to zero for newly converted particles. More recently, a similar analysis to [25] increased the generality of that result by rewriting $f(P_A(x,t))$ as $\beta(x,t)$ and including drift [26].

These integrodifferential approaches have very recently begun to be applied in the context of environmental solute transport, with a first order linear decay chain being considered in the context of plume development [27]. Whereas many theoretical results in the physics literature concerning anomalous transport focus on anomalous *diffusion* in particular (and are derived in the subdiffusive limit), the pre-asymptotic behavior of transport that will eventually become Gaussian is potentially more relevant in geophysical and environmental systems. In such systems, we consider transport in a biased, heterogeneous field that drives advection and dispersion in addition to diffusion. The CTRW is a useful tool for understanding the early time "anomalous dispersion" behavior (i.e., plume asymmetry) in such systems, and so adding reactions to the CTRW framework has the potential to be fruitful.

Motivated by this, we develop integrodifferential equations which describe reactive solute transport in natural media by adding a non-mass-conservative complication to the standard CTRW treatment to capture the behavior of the continuous movement of two species of particles, A and B, which are capable of chemically reacting with each other according to the irreversible reaction $A + B \to 0$. The connection of reaction to transport lies in the fact that particles must become sufficiently close in order to react.

The interplay of transport and reaction is relevant across scales, and we develop a scale-independent framework for incorporating reaction. We then consider two models of reactive solute transport that each apply at different scales, and write down the governing equations for both. A crucial point is the dependence of the mathematical formulation on the respective length scales at which transport and reactions are modeled. At the smaller ("microscopic") resolution, where both reaction and transport are modeled at the same scale and collocation of particles is taken to guarantee reaction, the equation is strongly nonlinear, and it is not apparent how to develop a generalized master equation with reactions. Considering a larger-scale ("mesoscopic") case, we introduce a latching upscaling scheme to upscale the treatment of transport and thereby essentially separate it from the small-scale motion which triggers reaction. This maneuver exploits the flexibility in what constitutes a "transition" in the context of continuously moving solute and also depends on certain assumptions about the temporal smoothness of P_A and P_B. This done, it is possible to straightforwardly obtain a mesoscopic integrodifferential master equation in the face of $A + B \to 0$ reactions.

From a theoretical point of view, we are especially interested in delineating the spatial distributions of the parent species A and B, and understanding how reaction affects their evolution over time. We show the effect of reaction is to reduce the amount of "memory" in the integrodifferential master equations, leading to particle distributions less anomalous than those which would develop in the same environment in the absence of reaction. We also manipulate the mesoscopic master equation and show how, in the case of pure advection and

diffusion, it collapses into the advection-dispersion-reaction equation (ADRE), and how, in the case of no reaction, it collapses into the familiar CTRW GME.

C. Numerical solution

So far, we have discussed equation formulation; ideally one wishes to obtain an analytical or numerical *solution*. Surprisingly, in light of the variety of bimolecular reactions considered and the large amount of relevant literature, the existing literature does not appear to treat mesoscopic CTRW for anomalous transport with bimolecular reactions between two species with *independent*, *spatially variant* concentrations.

In the absence of reaction, solution of the CTRW master equation is possible either by means of the Fourier-Laplace transformation [28] or, in a special case, by recognizing the CTRW's equivalence in the long time limit, for pure power law ψ, to the fractional diffusion equation (FDE) [17]. (The latter has a known solution in terms of Fox's H function.) In the presence of reaction, however, the governing equations are nonlinear and cannot be attacked with integral transforms. Analytic solutions *do* exist in the case of first-order irreversible $A \rightarrow B$ reactions [17] and reversible $A \rightleftharpoons B$ reactions where both species share the same power law ψ [29]. In these cases, it is relatively straightforward to modify the Green's function for unreactive transport to generate the Green's functions for A and B. However, analytic solutions do not seem to have been developed in other, more general cases.

Since we are working in a Eulerian realm, in the absence of analytic solutions for direct evaluation of the probability dynamics master equation, finite difference numerical techniques are desirable. For the special case of the FDE with a first-order decay (i.e., CTRW for unbiased transport, in the long time limit, with a pure power law ψ and a decay term outside the operator), numerical methods have been presented by [22] and others. Techniques also exist to account for biased operators [30]. However, it has been established in the case of pure decay [17], as we will show for bimolecular reactions, that in the domain of anomalous transport, reaction alters the transport operator. This breaks the correspondence of the CTRW to the fractional derivative operator, and so the relevance of these numerical methods to modeling reactive anomalous transport is unclear.

As the probability dynamics master equation for both unreactive and reactive transport is a Volterra partial integrodifferential equation (PIDE), it is also reasonable to consider general numerical techniques for these types of equations. In the numerical analysis literature, there appear to be some solution techniques for Volterra PIDE with certain forms of convolution kernel (e.g., [31]), but no general techniques for integration were found analogous to the many that exist for differential equations. Furthermore, in the authors' own explorations with finite difference schemes for biased transport operators (where the memory was summarized using a trapezoidal rule approximation), numerical stability came at the expense of excessively coarse spatial resolution, suggesting this may not be a promising avenue.

At present we are thus left, for general simulations, with Monte Carlo particle tracking. This Lagrangian approach generates stochastic realizations of the underlying CTRW transitions and reactions for a large number of particles, rather than integrating the Eulerian probability dynamics master equation. This technique has been widely used in the reactive transport literature with nearest neighbor transitions on a lattice and particle transitions drawn from a suitable ψ. The method is clearly described in [32]. For incorporating bimolecular reactions within a microscopic picture, the technique has been employed for pure diffusion by [3] and for power law ψ by [33]. It has also been used for monomolecular decay simulations (where there is no real distinction between micro- and mesoscopic) by [18]. For incorporating bimolecular reactions within a mesoscopic picture, it has been used for pure diffusion by [34] and for power law ψ by [33]. Particle tracking simulations of anomalous reactive transport have also been run without a lattice, where particles move freely in space and react probabilistically if within a certain proximity [35,36].

While Monte Carlo approaches are relatively simple to implement and have been used successfully by many authors, they do not provide direct numerical support for a given probability dynamics master equation. Given that we build up to a mesoscopic integrodifferential equation in which the transport operator is affected by reaction, going against some prior treatments, numerical support is invaluable. To support the Eulerian master equation, we develop a hybrid finite difference–particle tracking technique. We generate gridded data via a reactive mesoscopic particle tracking simulation, and then apply finite difference operations to the data which mimic both sides of our reactive integrodifferential master equation. By showing that these remain equal over time, we validate our equation while avoiding the numerical accuracy and stability problems that arise from time stepping finite difference numerical evaluation of a Volterra PIDE with a long memory.

II. MODIFIED JUMP DISTRIBUTIONS

Imagine that a solute particle of species S has a probability per unit time of another solute particle reacting with it (either because the other particle transitioned from another site, or because they have both been at the same site for a while, and they finally interact) when it is at location x at time t. Our objective is to modify the jump distributions $\psi_S(\Delta_x, \Delta_t)$ that are determined for species S (where S stands in for either A or B) in the absence of reaction. The calibrated jump distribution is mass-conservative, with all particles eventually jumping to some other site (which we always imagine as representing a small volume in space). This is to say that $\int_0^\infty \sum_{\Delta x} \psi_S(\Delta_x, \Delta_t) = 1$. We can thus handle reaction in a manner similar to that of Seki *et al.* [37], by modifying the jump distribution so that reacted particles are essentially permanently trapped. In the presence of reaction, $\int_0^\infty \sum_{\Delta x} \psi_S^*(\Delta_x, \Delta_t) < 1$.

For greater clarity: particles are imagined as moving continuously through space, which is partitioned into small, imaginary, disjoint volumes, each of which is considered a "site." Immediately, when a particle enters a new volume, it is considered to have completed a transition. In the context of solute transport, these transitions are essentially bookkeeping devices, and we do not imagine that particles are actually stationary for periods of time before making instantaneous

jumps. However, in porous and other natural media, the presence of slow and fast pathways means that transport is typically anomalous, necessitating the use of equations such as (1) and (2) to capture behavior rather than a simple advection-diffusion equation [1].

It is worth noting that because we have defined a transition as always *between* sites, our mathematical treatment of ψ^* does not distinguish particles that are stationary for all time from particles that react and are thus annihilated. However, the particles are constantly moving in any real system, and the probability that they remain within some finite volume for all time is zero, so we neglect this possibility.

We define the following statements:

(1) **M**: The particle arrives at volume x at time t' and *moves* to the volume centered at $x + \Delta x$ in the interval $[t' + \Delta_t, t' + \Delta_t + dt]$.

(2) **NL**: The particle *never leaves* the volume of its own accord during $[t',t' + \Delta_t]$.

(3) **NR**: The particle *never reacts* during $[t',t' + \Delta_t]$.

It follows that the jump distribution determined in the absence of reaction is defined $\psi_S(\Delta_x,\Delta_t)dt = \Pr(\mathbf{M},\mathbf{NL})$, and $\psi_S^*(\Delta_x,\Delta_t;x',t')dt = \Pr(\mathbf{M},\mathbf{NL},\mathbf{NR})$. We add the parameters x' and t' because **NR** generally depends on external factors which may vary across space and time. It seems reasonable to assume in a number of scenarios that **NR** is probabilistically independent of **M** and **NL**, so

$$\psi_S^* = \psi_S \times \Pr(\mathbf{NR}). \tag{3}$$

We define $T_S(x,\Delta t,t')$ to be the survival probability for a particle of type S, arriving at x at t' and remaining there for time Δt without reacting. Then, it follows that $\Pr(\mathbf{NR}) = T_S(x,\Delta_t,t')$, and that $T_S(x,t,t')$ satisfies the governing equation

$$\frac{dT_S}{dt}(x,t,t') = -\rho_S(x,t)T_S(x,t,t'), \tag{4}$$

where $\rho(x,t)$ is the probability rate of a given S particle reacting at exactly time t, which we will term the *extinction probability*. Then it follows that

$$T_S(x,\Delta_t,t') = \exp\left\{-\int_0^{\Delta_t}\rho_S(x,t'+\tau)d\tau\right\}, \tag{5}$$

and by substitution into (3) that

$$\psi_S^*(\Delta_x,\Delta_t;x',t') = \psi_S(\Delta_x,\Delta_t)\exp\left\{-\int_{t'}^{t'+\Delta_t}\rho_S(x',\tau)d\tau\right\}. \tag{6}$$

An analogous relationship exists for both species, where S stands in for either species A or B. Unlike the relationship for the reaction-free case, an absolute clock time t' figures as a variable as well, complicating analysis in Laplace space. Using the above modified transition distribution analysis, we develop (to different degrees) two approaches, one microscopic and one mesoscopic. Both are similar, but each employs different definitions for the extinction probabilities ρ_A and ρ_B and models transport with different transition lengths.

The *microscopic* approach is based on a reaction region approach [7]. We imagine discrete linear, square, or cubic volumes that fill space (respectively depending on the dimensionality of the system) centered on a lattice of sites, and *identify* them with the reaction regions (so in this approach, particle transition lengths are on the scale of the reaction "radius"). We stipulate reaction to occur (and occur instantaneously) if and only if an A and a B particle are simultaneously located in the same volume (i.e., "at the same site"). The particles are thought of as zero dimensional points, which are "at" the site corresponding to the volume they are within, and which make an instantaneous site-to-site transition at the instant they pass into an adjacent volume. The lattice is fine enough that most of its sites will be empty at any given time, a few will contain one particle, and fewer will contain two. Since reaction is taken as assured when two potentially reactive particles are at the same site, the probability of three different particles (of any combination of species) being simultaneously at the same site is implicitly taken to be negligible. In this approach, transitions are allowed to neighboring sites only.

The *mesoscopic* approach, by contrast, separates the scales of reaction and (potentially anomalous) transport. The transport (described by the CTRW equations) is modeled at the coarser of the two scales, where each site at the scale of the coarse lattice is taken to represent a volume much larger than a particle's reaction region. This conceptual picture allows for multiple A and B particles to be present at a given site at a given time, but imagines that there are at most negligible concentration gradients across any given volume at the coarse scale. The probability of reaction of a given A particle per unit time is taken to be proportional to the concentration of B particles at that site at that time, and vice versa. Again, transitions are allowed to neighboring sites only.

III. MODELING TRANSPORT AT MICROSCOPIC SCALE

We first consider a microscopic conception, in which the walkers are taken as analogs to individual reactant molecules, with reaction assured on collocation. The microscopic model is illustrated in Fig. 1. On this conception, we equate the probability rate of arrival of a B particle at a site containing an A particle with the probability rate of reaction, so $\rho_A(x,t) = R_B(x,t)$, [and similarly $\rho_B(x,t) = R_A(x,t)$]. This means that we write

$$\psi_A^*(\Delta_x,\Delta_t;x',t') = \psi_A(\Delta_x,\Delta_t)\exp\left\{-\int_{t'}^{t'+\Delta_t}R_B(x',\tau)d\tau\right\}. \tag{7}$$

The probability dynamics are described by two equations. The first is simply (2), where Ψ_A is replaced by

$$\Psi_A^*(\Delta_t;x',t') \equiv \left[1-\int_0^{\Delta_t}\psi_A(t)dt\right] \times\left[\exp\left\{-\int_{t'}^{t'+\Delta_t}R_B(x',\tau)d\tau\right\}\right]. \tag{8}$$

The second is the following recurrence relation:

$$[1+P_B(x,t)]R_A(x,t) = \sum_{x'}\int_0^t\psi_A^*(x-x',t-t';x',t')R_A(x',t')dt', \tag{9}$$

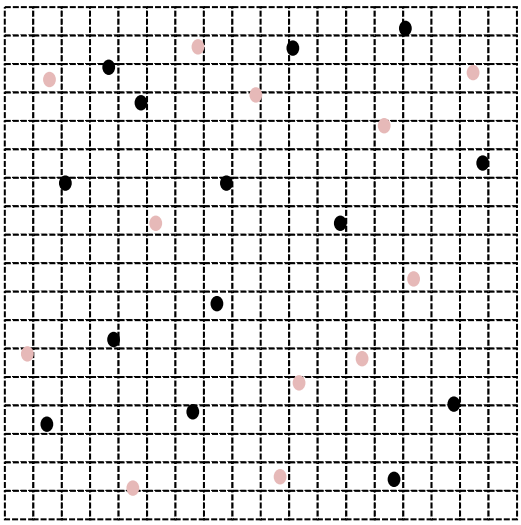

FIG. 1. (Color online) Schematic of A (black) and B (light-colored) particles undergoing CTRW relative to the volumes (each small square surrounded by dotted lines represents a volume) at the microscopic scale. Each particle is taken to be at the "site" located at the center of the volume that contains its centroid.

where the ψ_A^* accounts for A particles that have B particles arrive before they (the A particles) make their next transition, and the $[1 + P_B(x,t)]$ accounts for A particles that survive and then transition to sites that already contain B particles. In the microscopic scheme, each reaction occurs with one particle transitioning onto a site, and another particle already being there. So it is necessary to remove probability mass from the system both while the particle is waiting at a site x' (via the modified distribution ψ^*), and also immediately on arrival at a new site. If $\psi_A = \psi_B$ and the particles are initially randomly distributed, then around half the reactions that A particles participate in will be on account of their own transition, and half due to transition of a B particle (and vice versa). Thus, neither effect can generally be neglected. Because of the nonlinearity on the left-hand side (LHS) of (9), it is not clear how to combine the above relations into a single integrodifferential governing equation. We will not analyze this case further, but note that it has potential relevance for pore scale modeling and analysis of reactant segregation. It is also worth observing that [21] reported a qualitative difference in the form of integrodifferential probability dynamics equation in systems where there is a uniform decay rate while at a site versus in which reaction is triggered on transition. The microscopic conception involves both dynamics.

IV. UPSCALING FROM MICROSCOPIC TO MESOSCOPIC

In this section, we develop a general modeling approach that eliminates the fixed reaction region assumption and yields tractable equations, but at the cost of assuming some spatial smoothness of P_A and P_B that is not required in the microscopic approach. This mesoscopic conceptual approach models transport and reaction at two different length scales: transport is represented at a coarse scale by CTRW transition distributions ψ_A and ψ_B, and reaction is imagined as being driven by much finer-scale movements (as in the microscopic approach) and captured indirectly, by means of a mass action law. On this conception, we write $\rho_A(x,t) = \Gamma P_B(x,t)$ and $\rho_B(x,t) = \Gamma P_A(x,t)$, where P_A and P_B are understood as being defined at the coarse scale, and Γ is a spatially invariant rate constant representing the thermodynamics. Essentially, this amounts to the stipulation that $R_B(x,t)$ defined at the fine (i.e., microscopic) scale can be captured by the mass action term $\Gamma P_B(x,t)$ defined at the coarse scale. [Naturally, this relationship cannot apply for systems described by single scale CTRW equations, since the relationship (2) would then hold.] The separation of scales may seem somewhat artificial, but is actually natural for transport in heterogeneous media, where reaction rates are limited by diffusion between molecules which are in the same pore and anomalous transport is naturally captured over larger scales of heterogeneity. In homogeneous environments, the approach is still valid. In fact, regardless of whether there is a natural scale separation, it is possible to upscale the transport from a microscopic model.

The upscaling (which for simplicity we describe in one dimension) works by partitioning the microscopic lattice domain into regions with a grid of evenly spaced parallel lines, each with its own numeric index n. Mesoscopic "sites" are taken to correspond to these partition lines, and a transition to a new site is *defined* to have occurred the instant when when the cumulative effect of the walker's microscopic movements lead it to cross a partition line with an index different from n. We term this a *latched upscaling* scheme because we imagine the walker "latching" to site n when it crosses a partition line for the first time after being previously associated with site $n-1$ or site $n+1$, whereas subsequent movements across the same grid line prior to next arrival at site $n-1$ or site $n+1$ do not trigger a mesoscopic transition (although they of course correspond to transitions on a microscopic lattice). This upscaling approach is conceptually similar to the RP-CTRW approach recently introduced [38], except both forward and backward transitions are permitted.

Figure 2 illustrates the upscaling of a 2D microscopic lattice to a 1D mesoscopic lattice. The solute currently in the region corresponding to site n is shown. The regions represented by neighboring mesoscopic sites overlap, and each site of the coarse lattice is seen as representing a sort of microscopic model of the type discussed in the last section, with many A and B particles undergoing small transitions on a fine lattice. Again, the microscopic lattice is shown for the region corresponding to site n.

In general, all random walk models capture continuous movement by a series of discrete transitions, and so periodically "catch up" with an underlying process. Upscaling from a microscopic lattice to a coarser one, as illustrated, essentially amounts to catching up with a process less frequently. If done properly, the upscaled random walk still captures the same underlying process. Figure 3 illustrates latching over time in one dimension for upscaling a random walk model of an underlying process from a microscopic lattice to a coarser one (here, the microscopic movements may be thought of as corresponding to the vertical coordinates of any of the walkers seen in Fig. 2). Figure 3 shows the latched coarse-scale site coordinate corresponding to the fine-scale path via the line with gray shading underneath that makes instantaneous, unit-length jump transitions to nearest neighbor sites. By connecting these

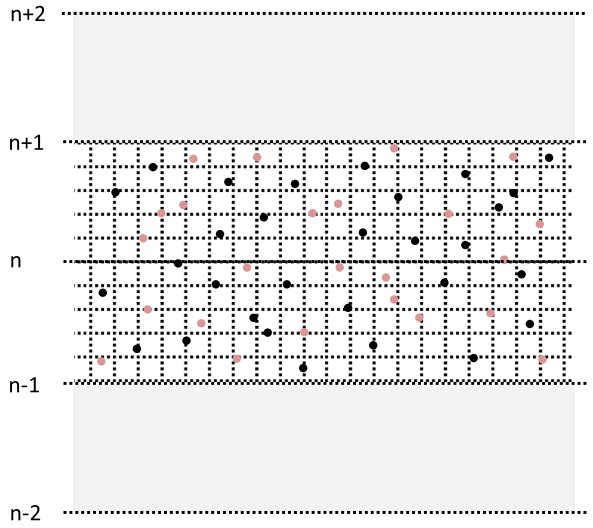

FIG. 2. (Color online) Schematic of the latched upscaling scheme whereby a two-dimensional (2D) microscopic picture is mapped onto a 1D mesoscopic picture. Each site (dotted, horizontal line) on the mesoscopic grid represents a surrounding volume in space that generally contains a number of particles of A and B, colored as in Fig. 1, and which could potentially be represented by a microscopic model. The microscopic model corresponding to site n is shown explicitly.

instantaneous jump transitions (with the dashed line), it is easy to see that a 1D upscaled model follows the same path as the fine-scale model, only it is forced to identify with the underlying process less frequently. This upscaling does not involve any additional mathematical or physical assumptions.

To generate higher-dimensional mesoscopic realizations, it is possible to treat each dimension with its own CTRW. Alternatively, a 2D mesoscopic lattice could be employed, however walkers that complete transitions to the same node may be at different nearby locations in space, so marginalization

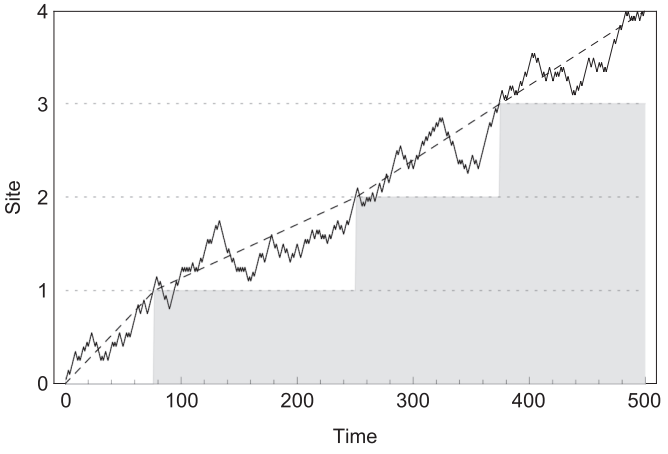

FIG. 3. Upscaling of a 1D CTRW (which can be imagined as the vertical coordinate of a single particle shown in Fig. 2) from microscopic to mesoscopic scales. Mesoscopic sites are indicated by horizontal dotted lines. A microscopic scale 1D random walk with a bias is shown (solid line), and its corresponding mesoscopic scale random walk is superimposed (dashed line). The current site index at the coarse scale over time is also shown (gray shading).

over these locations may be required to upscale ψ, and the exact correspondence of the mesoscopic CTRW to the microscopic one is not automatic. However, for our purposes it suffices to know that an upscaled transition is well-defined, and with regard to capturing *transport*, upscaled mesoscopic models may represent the behavior represented by microscopic models.

It is in capturing reaction that tradeoffs exist. As mentioned, a major advantage of the mesoscopic approach is that upscaled transitions play no role in triggering reaction not captured by Γ, so there is no need for the sort of nonlinearity seen on the LHS of (9), and in addition, the fixed reaction region assumption may be relaxed. However, we introduce the following assumptions in order to capture reaction with a mass action term:

(1) Over any volume represented by one site at the coarse scale, there are negligible gradients in the concentrations P_A and P_B; A and B are essentially uniformly distributed. This justifies the use of a fixed Γ.

(2) For adjacent sites x and x', $\Gamma P_S(x,t) \approx \Gamma P_S(x',t)$.

V. MODELING TRANSPORT AT MESOSCOPIC SCALE

A. CTRW analysis

Exploiting the scale separation arguments presented in the last section, we modify the transition distribution to take into account particles that are annihilated before they can move by writing

$$\psi_A^*(\Delta_x,\Delta_t;x',t') = \psi_A(\Delta_x,\Delta_t)\exp\left\{-\int_{t'}^{t'+\Delta_t}\Gamma P_B(x',\tau)d\tau\right\}. \quad (10)$$

Because the scale separation makes the role of mesoscopic transitions in triggering reaction negligible, we write the following general probability dynamics recursive relationship for R_A,

$$R_A(x,t) = \sum_{x'}\int_0^t \psi_A^*(x-x',t-t';x',t')R_A(x',t')dt', \quad (11)$$

which does not have nonlinearity on the LHS found in (9). Because of this, we can immediately exploit a result derived in [26] for *monomolecular* birth-death processes, given a suitable identification of their death rate with our upscaled mass-action law, $\rho(x,t)$ [$=\Gamma P_B(x,t)$]. (The authors mention in [34] that birth and death could be a result of reactions at a site, but this is never given explicit treatment, and anomalous bimolecular behavior is not analyzed further, either analytically or numerically.)

We thus arrive at the integrodifferential equation:

$$\frac{\partial P_A}{\partial t}(x,t) = \sum_{x'}\int_0^t \left[\phi_A(x-x',t-t')e^{-\int_{t'}^t \Gamma P_B(x',\tau)d\tau}P_A(x',t') - \phi_A(x'-x,t-t')e^{-\int_{t'}^t \Gamma P_B(x,\tau)d\tau}P_A(x,t')\right]dt' - \Gamma P_A(x,t)P_B(x,t). \quad (12)$$

An identical equation, with A and B subscripts permuted, obtains for species B. Here, the functions ϕ are those that would apply in the CTRW generalized master equation (GME) in the absence of reaction, defined as in the Laplace domain as (see [1])

$$\tilde{\phi}_A(\Delta_x,u) \equiv \frac{u\tilde{\psi}_A(\Delta_x;u)}{1-\sum_{x''}\tilde{\psi}_A(x'',u)}. \tag{13}$$

In the Appendix, we present an alternative derivation of (12) which is similar in spirit to the Scher-Lax characterization of the GME in the case of unreactive transport [1].

Equation (12) may be put in a more familiar GME form by defining transition functions ϕ_S^* based on the transition functions ϕ_S, multiplied by an exponential tempering factor to account for reaction:

$$\phi_A^*(\Delta_x,\Delta_t,x',t') \equiv \phi(\Delta_x,\Delta_t)e^{-\int_{t'}^{t'+\Delta_t}\Gamma P_B(x',\tau)d\tau}. \tag{14}$$

We imagine that there is a single special site at ∞ that probability mass is transferred to in the case of reaction, from which probability mass does not return in finite time. We abuse notation to write explicitly

$$\begin{aligned}\phi^*(\infty,\Delta_t;x',t') &= \delta(\Delta_t)\Gamma P_B(x',t')\ \forall x'\neq\infty,\\ \phi^*(-\infty,\Delta_t;\infty,t') &= 0.\end{aligned} \tag{15}$$

Then substituting these definitions into (12) we arrive at the following form of modified GME:

$$\begin{aligned}\frac{\partial P_A}{\partial t}(x,t) = \sum_{x'}\int_0^t [&\phi^*(x'-x,t-t';x,t')P_A(x,t')\\ &-\phi^*(x-x',t-t';x',t')P_A(x',t')]dt'.\end{aligned} \tag{16}$$

From the point of view of reactive solute transport, it is important to highlight the degree to which anomalous transport is affected by the reaction in (12); reaction is more than just an add-on to the unreactive GME. An interpretation of this equation is that the exponential decay factors damping the memory function reduce the number of A particles exchanged between neighboring sites to account for particles that reacted in the recent past and were removed from the probability mass balance before they made a transition to a new site, whereas the sink term represents A particles that are reacting presently at the current site x. Similar behavior has been seen previously in studies of reactive solute transport with subdiffusion and radioactive decay (with [17] observing that their approach was adaptable to multiparticle systems) as well as more general studies which include an arbitrary reaction rate function. Arguably the conclusion about the bidirectional interplay of transport and reaction has been implicit in some theoretical results going back at least to [23]. However, it is shown explicitly in the context of an $A+B\rightarrow 0$ reaction between two solute species.

B. Two special cases

1. The case of no reaction: Reduction to the standard CTRW GME

A check on the validity of the above formulation stems from the fact that if either there are no B particles or $\Gamma=0$, then there must be no reaction, and (12) must degenerate to the GME for the standard CTRW formulation. Substituting in either $P_B=0$ or $\Gamma=0$ immediately yields

$$\begin{aligned}\frac{\partial P_A}{\partial t}(x,t) = \sum_{x'}\int_0^t [&\phi_A(x'-x,t-t')P_A(x,t')\\ &-\phi_A(x-x',t-t')P_A(x',t')]dt',\end{aligned} \tag{17}$$

satisfying this requirement. Recall that, as claimed above, the ϕ are the same transition functions found in the GME for transport in the absence of reaction.

2. The case of exponential ψ_A: Reduction to the advection-diffusion-reaction equation

It is well established that when the temporal portion of the waiting probability distribution is exponential, the CTRW reduces to the form of the ADE. The standard modification of the ADE in the case of the two-component reaction is to add a sink term of the form $-\Gamma P_A(x,t)P_B(x,t)$ to represent the loss due to a chemical reaction, leading to the ADRE:

$$\frac{\partial P_A}{\partial t}(x,t) = -v\frac{\partial P_A}{\partial x}(x,t)+D\frac{\partial^2 P_A}{\partial x^2}(x,t)-\Gamma P_A(x,t)P_B(x,t). \tag{18}$$

It is interesting to see whether solution (12) can be placed into the same form. To do so, consider separable jump distributions of the form $\psi_A(x,t)=X(x)ke^{-kt}$. It is easy to show in this circumstance that $\phi_A(\Delta_x,\Delta_t)=X(\Delta_x)k\delta(\Delta_t)$. Then it follows from (12) that

$$\begin{aligned}\frac{\partial P_A}{\partial t}(x,t) = k\sum_{x'}[&X(x'-x)P_A(x,t)-X(x-x')P_A(x',t)]\\ &-\Gamma P_A(x,t)P_B(x,t).\end{aligned} \tag{19}$$

Given nearest neighbor transitions on a 1D lattice with spacing Δ_x, we may divide the transition probability into a symmetric, diffusive part $[S(x)=\frac{X(x)+X(-x)}{2}]$ and an asymmetric, advective part $[A(x)=\frac{X(x)-X(-x)}{2}]$, so $X(\Delta_x)=S(\Delta_x)+A(\Delta_x)$. We may then write (19) as

$$\begin{aligned}\frac{\partial P_A}{\partial t}(x,t) = &kA(\Delta_x)[P(x+\Delta_x,t)-P_A(x-\Delta_x,t)]\\ &-kS(\Delta_x)[P(x+\Delta_x,t)-2P_A(x,t)\\ &+P_A(x-\Delta_x,t)]-\Gamma P_A(x,t)P_B(x,t).\end{aligned} \tag{20}$$

By defining $v=-kA(\Delta_x)\Delta_x/2$ and $D=-kS(\Delta_x)\Delta_x^2$, we arrive, for small Δ_x, at (18), the ADRE.

We saw above, in (12), that an increasing rate of reaction corresponds to weaker memory, approaching a pure ADRE in the limit. It is further apparent from our analysis here that when the ψ function is chosen to correspond to memoryless conditions in the unreactive case that it leads to a memoryless condition in the presence of reaction, also. These observations have a reasonable interpretation. Our mesoscopic analysis imposes a uniform rate of reaction per unit time that is shared by all particles in a volume (i.e., particles are exchangeable and decay is essentially exponential over any short interval). Reaction acts to make the effective solute transport less anomalous by preferentially killing off particles that are waiting a long time to make a transition, relative to particles

that transition quickly. However, when ψ is exponential, there is also a uniform-per-unit-time probability that any particle in the volume will leave the volume, independent of its history. In that case, both transport and reaction are logically decoupled processes, and this is reflected in the mathematics as well.

VI. NUMERICAL CORROBORATION

In the above, we presented a closed-form, time-domain mesoscopic scale equation for anomalous transport undergoing $A + B \to 0$ reaction by employing an approximation about the spatial smoothness of the solutions for both species. Since the form of the equation differs from some previous treatments in which reaction and transport were treated by entirely separate terms, it is desirable to numerically corroborate this approximation, and also to support our qualitative conclusions about the interplay of transport and reaction in (12).

Since integrodifferential equations with long memory, such as (12), are difficult to evaluate in the time domain, we develop an indirect approach to corroborate the solution. Essentially the technique is this:

(1) Perform a reactive particle tracking simulation on a lattice where transitions for each species are chosen according to the appropriate ψ_S, and reactions according the appropriate ρ_S. For each species, $P_S(x,t)$ is recorded over time in a concentration data matrix M_S, whose rows represent spatial locations and whose columns represent successive times.

(2) Compute an approximation matrix L, corresponding to the LHS of the integrodifferential equation being examined [in our case, we consider each of (12) and (17)] by applying a temporal differentiation matrix D_t, so $L \equiv D_t M_A$.

(3) Compute an approximation matrix R to the right-hand side (RHS) of the integrodifferential equation being examined by applying a spatial difference matrix D_x and a temporal integration operator. In the case of (17), where the integral kernel ϕ is independent of x and t, it is possible to represent the integration operator as an upper triangular banded matrix K, so $R \equiv D_x M_A K$. In the case of (12), the kernel is dependent on space and time, so the integration cannot be represented as a matrix operation; it must be done procedurally.

(4) Compare the the numerically computed L and R. To the extent that their entries are the same at a given row and column (location and time, respectively), the validity of the integrodifferential master equation is confirmed for the chosen ψ_A and ψ_B.

Here we consider a simple CTRW in one dimension, which can be thought of as representing advective transport of solute in heterogeneous media. A series of imaginary, infinite, evenly spaced parallel planes correspond to the coarse-scale sites in the development above. In this case, a transition is deemed to have occurred on arrival of a solute particle at a given plane, and advection to be a strong enough process that transitions occur in the down-gradient direction, only.

The algorithm begins at time $t = 0$, and each particle has its time of next transition (to a subsequent plane) computed in Monte Carlo fashion by drawing from the appropriate ψ_S. Subsequently, the computer iteratively takes small time steps of length Δ_t until some final value of t is reached. Particles that have their next transition time during the present time step are moved accordingly, and have their time of next transition recomputed. Also during each step, at each site x, the reaction probability $k_A(x,t)$ for any A particle is determined by multiplication of a fixed constant Γ, by Δ_t, by the number of B particles at that site at time t, divided by the number of B particles in the system when $t = 0$. For each A particle, a uniform random variable on the interval $[0,1]$ is drawn. If this number is less than $k_A(x,t)$, that particle is removed from the simulation. An identical process is performed for the B particles. (Because the spatial units are never specified, neither are the spatial units of Γ; the only important fact is that increasing Γ increases the reaction rate, all else being equal.)

In our particular simulation, we assume that the transition distribution for both species is the same one-sided (i.e., $\beta = 1$) stable distribution, so $\psi_A(t) = \psi_B(t) \sim S(\alpha,\beta,\mu,\sigma)$, where the parametrization $\alpha = 0.8$, $\beta = 1.0$ $\mu = 2.0$, and $\sigma = 1.0$ was chosen. This distribution is defined by its Laplace transform,

$$\tilde{\psi}_S(u) = \exp\{-(\sigma u)^\alpha/\cos(\pi\alpha/2) - \mu u\}, \qquad (21)$$

which may be used to directly compute the transition functions for the CTRW, and also directly inverted to check the validity of the Monte Carlo generator used (the Math.NET numerics package), as shown in Fig. 4. We use 50 sites, connected in a ring. Given this topology, there is no gain or loss of mass at any boundaries (as there are no boundaries); all mass loss is due to reaction. Initially, 50 000 particles of A were located at the site with index 1, and 50 000 particles of B were uniformly distributed across all the sites. Advection was permitted to occur exclusively in the direction of increasing site index (i.e., each transition was to a site whose index was one higher, or from site 50 to site 1). The simulation was run $t = 300$, with $\Delta_t = 0.1$, where both quantities are in arbitrary units, consistent with those used to define ψ_A and Γ. Our simulation ended before any significant amount of A reached the largest index site, so the predictions are indistinguishable from what would be seen in an infinite domain. A schematic of the system, with its initial condition shown, is given in Fig. 5.

We began with a test in the case of unreactive A and B ($\Gamma = 0$) to establish the validity of the memory function

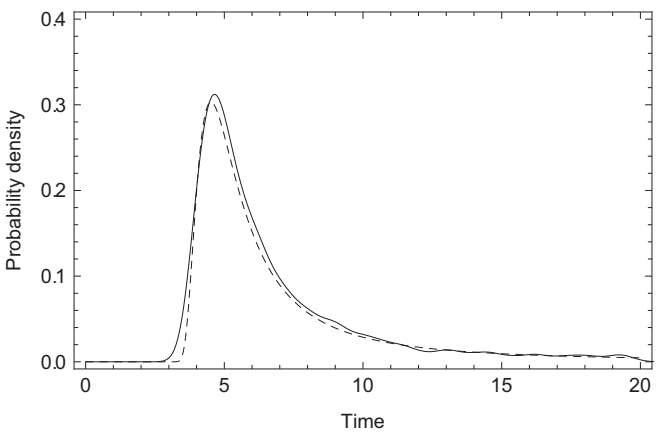

FIG. 4. Stable distribution, $S(0.8,1.0,2.0,1.0)$, as drawn Monte Carlo fashion (solid curve; a smoothed histogram is shown), and directly computed from inverting the Laplace transform (dashed curve).

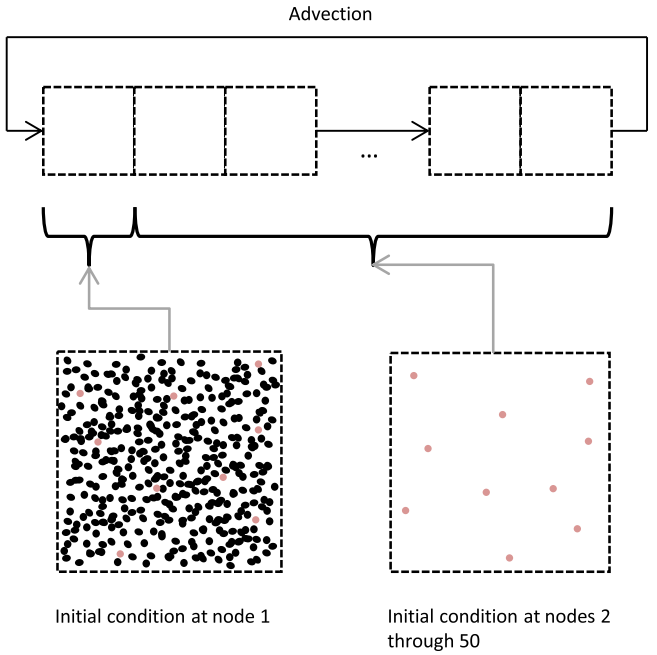

FIG. 5. (Color online) Schematic of site arrangement, direction of transport, and initial conditions in the numerical simulations. As in other schematics, A particles are black and B particles are light-colored.

which was computed using (21) and establish a baseline for the amount of noise in the numerical simulations]since in this case, the governing equations are the known-to-be-accurate CTRW equations (1) and (2)]. In the case of no reaction, we can visualize the actual evolution of the concentration in one spatial dimension and time as the surface plot shown in Fig. 6. Application of the procedure outlined above was used to generate L and R matrices. From these, temporal evolution at three different locations is shown in Fig. 7.

The analysis of the case of reactive A and B ($\Gamma = 4.5$) proceeded in a similar fashion. Figure 8 shows the actual evolution of the concentration in one spatial dimension and time for each of species A and B as surface plots. Application

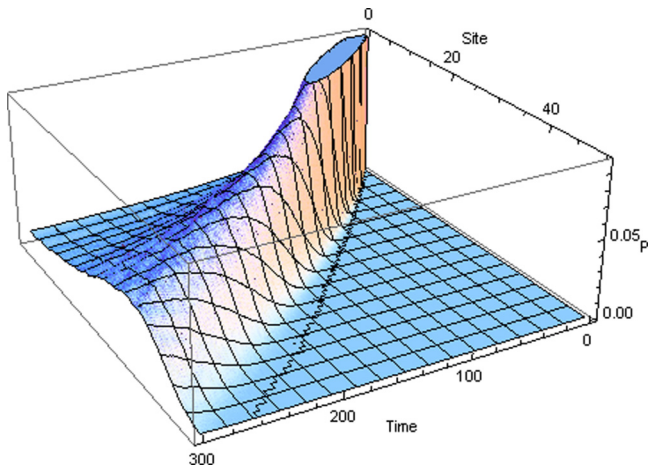

FIG. 6. (Color online) Surface plot showing the evolution of the concentration of A through space, over time in the unreactive case.

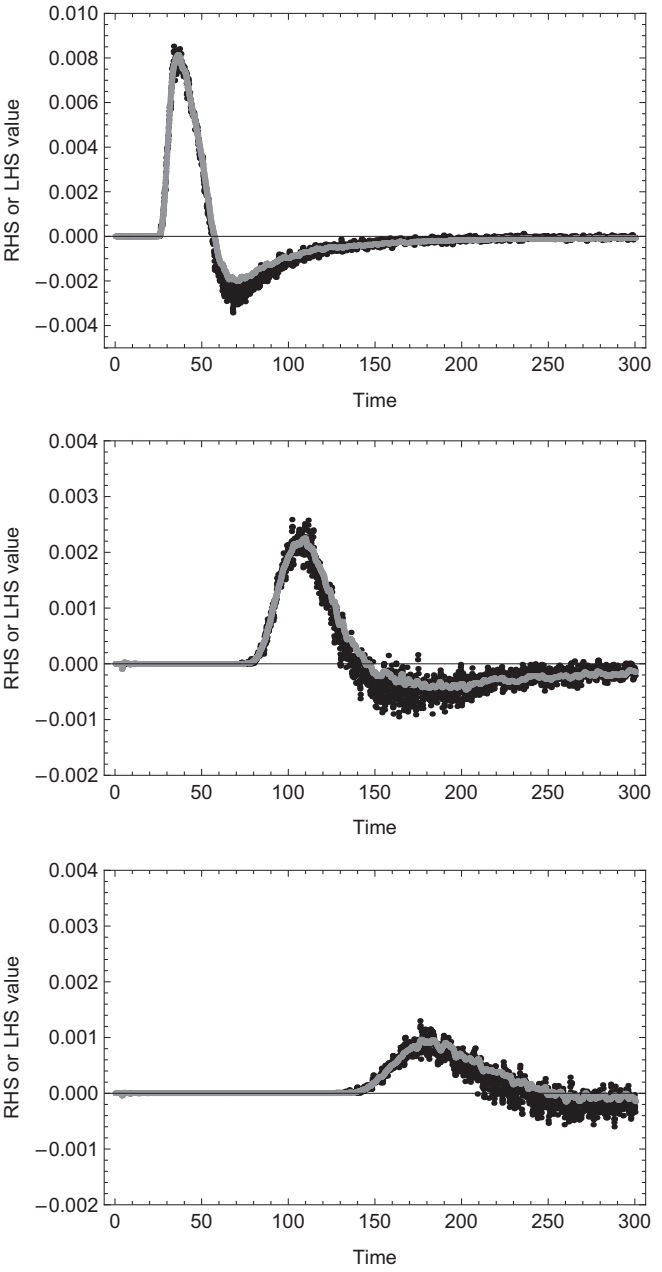

FIG. 7. Comparison of numerical computation of LHS (black points) and RHS (gray points) of (17) over time from Monte Carlo simulation data at location $x = 10$ (top), $x = 20$ (middle), and $x = 30$ (bottom).

of the procedure outlined above was used to generate L and R matrices. From these, temporal evolution at three different locations is shown in Fig. 9, which allows an assessment of our simplifying assumption. Coherence between L and R is generally quite good—on par with what is seen in the known-accurate unreactive case—providing corroboration of our analysis.

Another informative way to look at the data is to compare the Monte Carlo–generated plumes of A at the last time of each simulation: reactive and unreactive. These are shown on the same axes in Fig.10. It is apparent from examination of (12) that greater rates of reaction should reduce the temporal

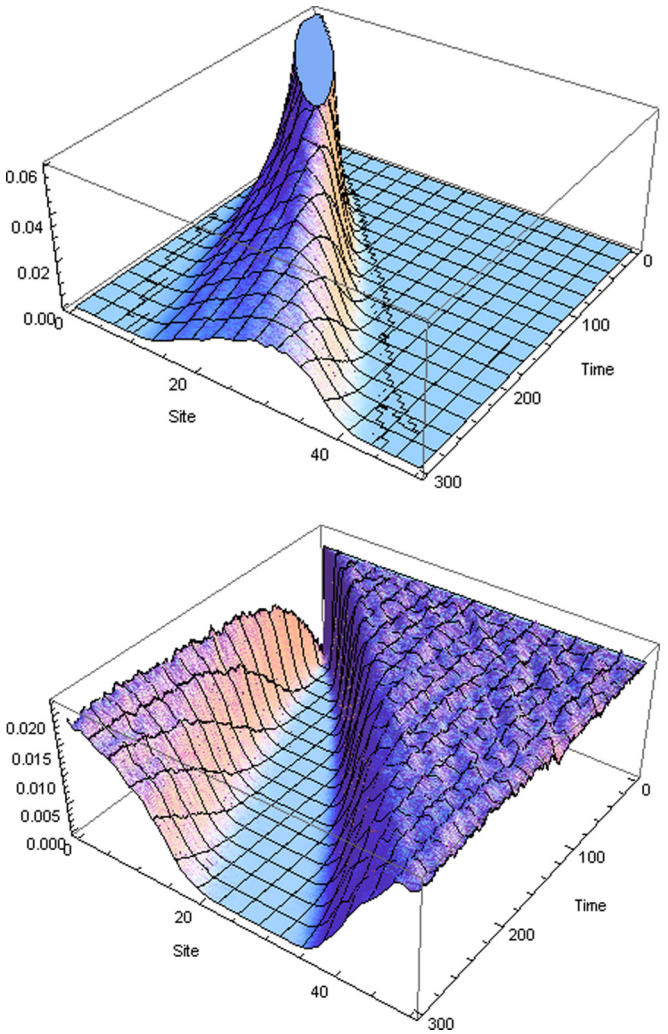

FIG. 8. (Color online) Surface plots of concentrations of species A (top) and species B (bottom).

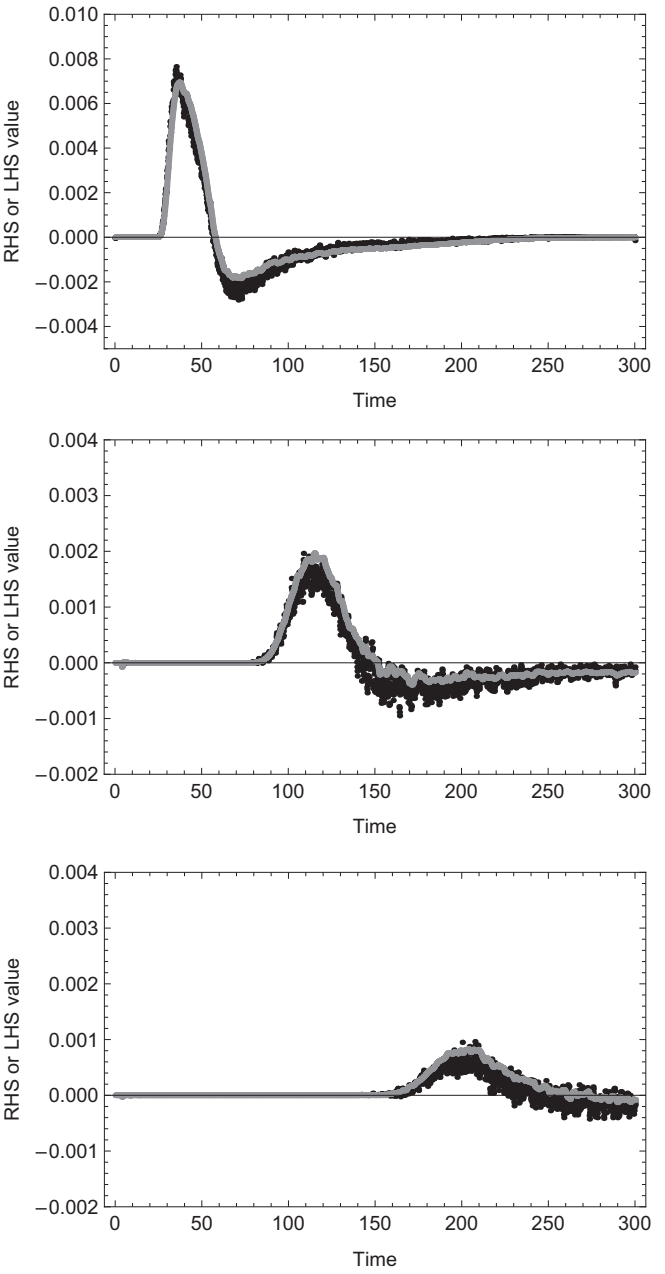

FIG. 9. Comparison of numerical computation of LHS (black points) and RHS (gray points) of (12) over time from Monte Carlo simulation data at location $x = 10$ (top), $x = 20$ (middle), and $x = 30$ (bottom).

support of the memory function ϕ^*, and make transport less anomalous. Indeed, this is exactly what is seen by comparison of concentration profiles. Since there was an instantaneous local release of species A, the concentration profiles can be seen as representative on the propagator for A. In the presence of reaction the results are seen to be, in fact, more Gaussian.

VII. SUMMARY AND CONCLUSIONS

In this paper, we analyzed $A + B \to 0$ reactions mathematically in the context of reactive solute transport. Two approaches to developing the CTRW governing equations were formulated at different scales, and the dependence of the equation form on the respective characteristic lengths at which reaction and transport are modeled was demonstrated. The first approach, at the microscopic scale, equates reaction with two potentially reactive particles being simultaneously at a site. This yields highly nonlinear CTRW recurrence relationships that are not obviously tractable: at this scale, there is a tight, two-way coupling between reaction and transport. Reaction can prevent particles from making transitions (which is inescapable) but in addition, transitions play a significant role in *triggering* reactions.

To yield a more tractable system, we developed an approach for scale separation of reaction and anomalous transport which makes the coupling one-way. Thus scale-separated, a mesoscopic approach easily yields an effective integrodifferential governing equation, showing the interplay of reaction and transport for each of the species (12). We then proceeded to corroborate the integrodifferential probability dynamics master equation using numerical simulations. Because it is difficult to numerically implement equations of this sort using finite difference time stepping, we developed an indirect

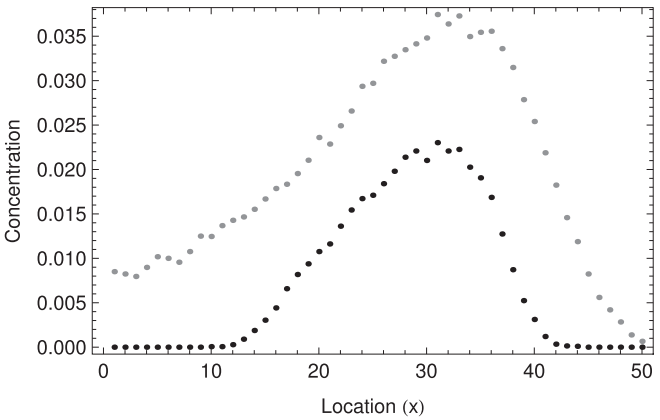

FIG. 10. Comparison of concentration of A at each site when $t = 300$ in the unreactive simulation (gray points) and the reactive simulation (black points), for the same initial conditions.

approach—one that may be applied more broadly to spatial evolution problems with memory.

The modifications in the mesoscopic integrodifferential governing equation we arrived at all have an intuitive basis relative to the standard CTRW solution:

(i) The exponential decay factors damping the transition function ϕ essentially reduce the amount of A particles exchanged between neighboring sites to account for particles that reacted in the recent past and were removed from the probability mass balance before they made a transition to a new site.

(ii) The sink term represents A particles that are reacting at the current moment, and which are then removed from the system.

Overall, we see from both analytical concerns and numerical results that an increasing reaction rate leads to a shorter "memory" than would otherwise be experienced by unreactive particles in the same system. This is consistent with what is found in monomolecular studies of particles undergoing subdiffusion subject to time-homogeneous first-order decay [17], and with arbitrary decay rates which may be dependent on space and time [26]. We also see that this solution degenerates into either an ADE or an ADRE under conditions where it would be expected to do so on physical grounds. Strikingly, the integrodifferential governing equation does not generally take an advection-dispersion-reaction form, because the reaction directly affects the memory of the transition function by preferentially eliminating particles with long site-residency times. Equally important is the realization that the length scales at which reaction and transport are modeled determine whether it is even possible to develop an integrodifferential probability dynamics equation analogous to the (unreactive) generalized master equation.

We conclude that from the point of view of reactive solute transport modeling, it is generally not adequate to place a second-order reaction term onto the generalized master equation for the same solute in the absence of reaction; the more involved equation we present here is required. This has not generally been appreciated in the literature.

ACKNOWLEDGMENTS

S.H. gratefully acknowledges the support of a postdoctoral fellowship from the Azrieli Foundation. B.B. gratefully acknowledges the support of a research grant from the Weizmann - UK Joint Research Program.

APPENDIX

In the main body of the work, we exploited a result derived for monomolecular anomalous transport with a general, space-and-time-dependent decay rate [26] to arrive at our mesoscopic GME. In this Appendix, we present an alternative derivation that differs from that presented in the main text, and which the reader who is familiar with the classic Scher-Lax [28] CTRW derivation for unreactive transport may find intuitive. We begin from (11). This relationship has the benefit of not requiring a nonlinear term on the LHS as in the microscopic case, since the role of transitions in triggering reaction is negligible in the two-scale, mesoscopic picture. Substitution of (10) into (11), multiplying both sides by $\exp\{\int_0^t \Gamma P_B(x,\tau)d\tau\}$, and using the idea that $\Gamma P_B(x,t) \approx \Gamma P_B(x',t)$ for nearest neighbor sites x and x' leads to

$$\left[e^{\int_0^t \Gamma P_B(x,\tau)d\tau} R_A(x,t)\right] = \sum_{x'} \int_0^t \psi_A(x-x',t-t') \times [e^{\int_0^{t'} \Gamma P_B(x',\tau)d\tau} R_A(x',t')]dt'. \quad \text{(A1)}$$

To simplify analysis, we make the following definitions:

$$\mathscr{R}(x,u) \equiv \mathcal{L}\left\{e^{\int_0^t \Gamma P_B(x,\tau)d\tau} R_A(x,t)\right\}(u), \quad \text{(A2)}$$

$$\mathscr{P}(x,u) \equiv \mathcal{L}\left\{e^{\int_0^t \Gamma P_B(x,\tau)d\tau} P_A(x,t)\right\}(u). \quad \text{(A3)}$$

Laplace transforming (A1) yields

$$\mathscr{R}(x,u) = \sum_{x'} \tilde{\psi}_A(x-x',u)\mathscr{R}(x',u), \quad \text{(A4)}$$

where $\tilde{\psi}_A$ is the Laplace transform of ψ_A. To relate R to P, we employ (2).

When defining ψ^* in (10), we noted the independence of the two processes leading to the solute particle's removal from its current (coarse-scale) site: departure to an adjacent (coarse-scale) site and reaction (a fine-scale process). With this in mind, we define the probability that a particle which arrives at x' at t' is still there after Δ_t in the presence of reaction as

$$\Psi_A^*(\Delta_t;x',t') \equiv \left[1 - \int_0^{\Delta_t} \psi_A(t)dt\right] \times \left[\exp\left\{-\int_{t'}^{t'+\Delta_t} \Gamma P_B(x',\tau)d\tau\right\}\right]. \quad \text{(A5)}$$

Substituting this modified Ψ_A^* (with its explicit dependence on space and time) into (2) in place of Ψ_A, Laplace transforming,

and then substituting (A2) and (A3) yields

$$\mathscr{P}(x,u) = \frac{1 - \sum_x \tilde{\psi}_A(x,u)}{u} \mathscr{R}(x,u). \tag{A6}$$

It is possible to exactly use the classic analysis for deriving the CTRW GME in the absence of reaction [1, Appendix A] to combine (A4) and (A6) into an equation exclusively in $\mathscr{P}$. Doing this yields the result

$$u\mathscr{P}(x,u) = \sum_{x'} \frac{u\tilde{\psi}_A(x - x',u)}{1 - \sum_{x''} \tilde{\psi}_A(x'',u)} \mathscr{P}(x',u) - \sum_{x'} \frac{u\tilde{\psi}_A(x' - x,u)}{1 - \sum_{x''} \tilde{\psi}_A(x'',u)} \mathscr{P}(x,u). \tag{A7}$$

Substituting (13) and (A3) into (A7) and then inverting the Laplace transform yields

$$\frac{\partial}{\partial t}\left\{e^{\int_0^t \Gamma P_B(x,\tau)d\tau} P_A(x,t)\right\} = \sum_{x'} \int_0^t \left[\phi_A(x - x',t - t')e^{\int_0^{t'} \Gamma P_B(x',\tau)d\tau} P_A(x',t') - \phi_A(x' - x,t - t')e^{\int_0^{t'} \Gamma P_B(x,\tau)d\tau} P_A(x,t')\right]dt'. \tag{A8}$$

Expanding the derivative on the LHS via the product rule, multiplying both sides by $e^{-\int_0^t \Gamma P_B(x,\tau)d\tau}$, and again using the idea that $\Gamma P_B(x,t) \approx \Gamma P_B(x',t)$ for nearest neighbor sites x and x' yields (12).

[1] B. Berkowitz, A. Cortis, M. Dentz, and H. Scher, Rev. Geophys. **44**, RG2003 (2006).
[2] A. Ovchinnikov and Y. Zeldovich, Chem. Phys. **28**, 215 (1978).
[3] D. Toussaint and F. Wilczek, J. Chem. Phys. **78**, 2642 (1983).
[4] M. W. Deem and J.-M. Park, Phys. Rev. E **57**, 2681 (1998).
[5] J.-M. Park and M. W. Deem, Phys. Rev. E **57**, 3618 (1998).
[6] A. Paster, D. Bolster, and D. A. Benson, Water Resour. Res. **49**, 1 (2013).
[7] S. K. Hansen, H. Scher, and B. Berkowitz, Adv. Water Resour. **69**, 146 (2014).
[8] S. B. Yuste, L. Acedo, and K. Lindenberg, Phys. Rev. E **69**, 036126 (2004).
[9] V. A. Volpert, Y. Nec, and A. A. Nepomnyashchy, Philos. Trans. R. Soc. A **371**, 20120179 (2013).
[10] D. Froemberg, H. H. Schmidt-Martens, I. M. Sokolov, and F. Sagués, Phys. Rev. E **83**, 031101 (2011).
[11] D. Bolster, D. A. Benson, T. Le Borgne, and M. Dentz, Phys. Rev. E **82**, 021119 (2010).
[12] D. Bolster, D. A. Benson, M. M. Meerschaert, and B. Baeumer, Physica A **392**, 2513 (2013).
[13] G. M. Porta, M. Riva, and A. Guadagnini, Adv. Water Resour. **35**, 151 (2012).
[14] G. M. Porta, S. Chaynikov, J.-F. Thovert, M. Riva, A. Guadagnini, and P. M. Adler, Adv. Water Resour. **62**, 243 (2013).
[15] D. Campos and V. Méndez, Phys. Rev. E **80**, 021133 (2009).
[16] G. Hornung, B. Berkowitz, and N. Barkai, Phys. Rev. E **72**, 041916 (2005).
[17] I. M. Sokolov, M. G. W. Schmidt, and F. Sagués, Phys. Rev. E **73**, 031102 (2006).
[18] A. Zoia, Phys. Rev. E **77**, 041115 (2008).
[19] M. G. W. Schmidt, F. Sagués, and I. M. Sokolov, J. Phys.: Condens. Matter **19**, 065118 (2007).
[20] E. Abad, S. B. Yuste, and K. Lindenberg, Phys. Rev. E **81**, 031115 (2010).
[21] B. I. Henry, T. A. M. Langlands, and S. L. Wearne, Phys. Rev. E **74**, 031116 (2006).
[22] A. Yadav and W. Horsthemke, Phys. Rev. E **74**, 066118 (2006).
[23] M. O. Vlad and J. Ross, Phys. Rev. E **66**, 061908 (2002).
[24] V. P. Shkilev, J. Exp. Theor. Phys. **109**, 852 (2009).
[25] S. Fedotov, Phys. Rev. E **81**, 011117 (2010).
[26] C. N. Angstmann, I. C. Donnelly, and B. I. Henry, Math. Modell. Nat. Phenom. **8**, 17 (2013).
[27] D. K. Burnell, J. W. Mercer, and C. R. Faust, Water Resour. Res. **50**, 1260 (2014).
[28] H. Scher and M. Lax, Phys. Rev. B **7**, 4491 (1973).
[29] T. A. M. Langlands, B. I. Henry, and S. L. Wearne, Phys. Rev. E **77**, 021111 (2008).
[30] W. Deng, J. Comput. Phys. **227**, 1510 (2007).
[31] I. Patlashenko, D. Givoli, and P. Barbone, Comput. Methods Appl. Mech. Eng. **190**, 5691 (2001).
[32] E. Heinsalu, M. Patriarca, I. Goychuk, G. Schmid, and P. Hänggi, Phys. Rev. E **73**, 046133 (2006).
[33] H. H. Schmidt-Martens, D. Froemberg, I. M. Sokolov, and F. Sagués, Phys. Rev. E **79**, 041135 (2009).
[34] C. N. Angstmann, I. C. Donnelly, and B. I. Henry, Phys. Rev. E **87**, 032804 (2013).
[35] Y. Edery, H. Scher, and B. Berkowitz, Water Resour. Res. **46**, W07524 (2010).
[36] D. Ding, D. A. Benson, A. Paster, and D. Bolster, Adv. Water Resour. **53**, 56 (2013).
[37] K. Seki, M. Wojcik, and M. Tachiya, J. Chem. Phys. **119**, 7525 (2003).
[38] S. K. Hansen and B. Berkowitz, Adv. Water Resour. **74**, 54 (2014).